Available online at www.sciencedirect.com
ScienceDirect
Mechanism and Machine Theory 42 (2007) 1418–1443
Mechanism and Machine Theory
www.elsevier.com/locate/mechmt

Multi-objective design optimisation of rolling bearings using genetic algorithms

Shantanu Gupta [a], Rajiv Tiwari [b,*], Shivashankar B. Nair [a]

[a] Department of Computer Science and Engineering, Indian Institute of Technology Guwahati, Guwahati 781039, Assam, India
[b] Department of Mechanical Engineering, Indian Institute of Technology Guwahati, Guwahati 781039, Assam, India

Received 8 March 2006; received in revised form 6 September 2006; accepted 2 October 2006
Available online 28 December 2006

Abstract

The design of rolling bearings has to satisfy various constraints, e.g. the geometrical, kinematics and the strength, while delivering excellent performance, long life and high reliability. This invokes the need of an optimal design methodology to achieve these objectives collectively, i.e. the multi-objective optimisation. In this paper, three primary objectives for a rolling bearing, namely, the dynamic capacity (C_d), the static capacity (C_s) and the elastohydrodynamic minimum film thickness (H_{min}) have been optimized separately, pair-wise and simultaneously using an advanced multi-objective optimisation algorithm: NSGA II (non-dominated sorting based genetic algorithm). These multiple objectives are performance measures of a rolling bearing, compete among themselves giving us a trade-off region where they become ''simultaneously optimal'', i.e. Pareto optimal. A sensitivity analysis of various design parameters has been performed, to see changes in bearing performance parameters, and results show that, except the inner groove curvature radius, no other design parameters have adverse affect on performance parameters.

Keywords: Rolling bearings; Multi-objective evolutionary optimisation; NSGA II; Mechanical design; Sensitivity analysis

1. Introduction

Rolling bearings are widely used as an important component in the most of the mechanical and aerospace engineering applications. Be it development of the house-hold appliance, automotive, space, aeronautical, micro- or nano-machine applications, all of them have given a boost to the advancement in the design technology of rolling bearings. This motivated design engineers to come up with a design technology that gives long lasting, more efficient and highly reliable bearing designs. These objectives are hard to satisfy, thus making it a numerically challenging problem. Furthermore, there is a need to optimize them collectively. The numerical toughness and a need to optimize them collectively warrant an application of the evolutionary multi-objective optimisation. Objective functions for optimisation are the dynamic capacity (C_d), the static

* Corresponding author. Tel.: +91 361 258 2667; fax: +91 361 269 0762.
E-mail addresses: gshantanu@gmail.com (S. Gupta), rtiwari@iitg.ernet.in (R. Tiwari), sbnair@iitg.ernet.in (S.B. Nair).

0094-114X/$ - see front matter © 2006 Elsevier Ltd. All rights reserved.
doi:10.1016/j.mechmachtheory.2006.10.002

capacity (C_s) and the elastohydrodynamic minimum film thickness (H_{min}). Due to the aforementioned toughness of the problem, there have been very few attempts at optimizing these objectives, simultaneously.

Several research works have been reported on optimisation of various machine elements, however, very few literatures are available on the optimisation of rolling bearings. Asimow [1] used the Newton–Raphson method for the optimum design of the length and the diameter of a journal bearing, which was supporting a given load at a given speed. The objective function was to minimize a weighted sum of the frictional loss and the shaft twist. Seireg and Ezzat [2] utilized a gradient-based search to optimise the bearing length, the radial clearance and the average viscosity of the lubricant. The objective function was chosen to minimize a weighted sum of the quantity of lubricant fed to the bearing and its temperature rise. Maday [3] and Wylie and Maday [4] used bounded variable methods of the calculus of variable, to determine the optimum configuration for hydrodynamic bearings. The design criterion was chosen that to maximize the load carrying capacity of the bearing. Seireg [5] reviewed some illustrative examples of the use of optimisation techniques, in the design of mechanical elements and systems. These include gears, journal bearings, rotating discs, pressure vessels, shafts under bending and torsion, beams subjected to the longitudinal impact and problems of the elastic contact and load distributions. Hirani et al. [6] proposed a design methodology for an engine journal bearing. The procedure of selection of the diametral clearance and the bearing length was described by limiting the minimum film thickness, the maximum pressure and the maximum temperature. All the aforementioned literatures were concerned mainly with the journal bearing design. However, internal geometries of journal bearings are far simple as compared to rolling bearings.

Changsen [7] described a design method by using a gradient-based numerical optimisation technique for rolling bearings. He proposed, five objective functions for design of rolling bearings: the maximum fatigue life, the maximum wear life, the maximum static load rating, the minimum frictional moment and the minimum spin to roll ratio. The concept of optimisation of the multi-objective of rolling bearings was also proposed. Only the basic concepts and solution techniques of an optimisation problem were introduced without any illustrations. Objective functions proposed for optimisation of rolling bearings are nonlinear in nature, moreover, associated with the geometric and kinematics constraints. Choi and Yoon [8] used GAs in optimizing the automotive wheel-bearing unit, by considering the maximization of life of the unit as the objective function. Periaux [9] discussed in detail the application of GAs to the aeronautics and turbo machineries. Chakraborthy et al. [10] described a design optimisation problem of rolling element bearings with five design parameters, by using GAs based on requirements of the longest fatigue life. They presented bearing internal geometrical parameters resulted from the optimised design of different bearing boundary dimensions. Main limitations of the method were that the use of the single objective function and some of constraints were unrealistic. Assembling angles were assumed and values of other constraint constants were chosen (arbitrary) fixed to solve the optimisation problem. Recently, Rao and Tiwari [11] developed a rolling bearing design methodology with the improved and realistic constraints for the single objective optimisation with the help of GAs.

A work on the multi-objective optimisation for the design of rolling bearings [12] does a weighted combination of these individual objective functions namely – the dynamic capacity, the static capacity and the minimum film thickness. The multi-objective problem is converted into a scalar optimisation problem. This work made use of the deterministic as well as stochastic algorithms, for solving the constraint scalar optimisation problem. As the deterministic approach the interior penalty function method was used, while the simulated annealing and genetic algorithms were used as stochastic approaches. This way of combining the multiple 'competing' objectives and optimisation of the obtained scalar objective has some prominent disadvantages – (1) a single run of the algorithm will give only one trade-off point, (2) solution points on a non-convex trade-off front cannot be obtained, and (3) no criteria for choosing weights for each of the objective function exists. The work proposed in this paper handles each of these problems.

Any weight based combination approach has drawbacks like unknown selection of weights for different objectives, one point obtained in one run, and incapability to explore non-convex regions of the trade-off front, i.e. *Pareto front*. Thus there is need to use a better multi-objective (evolutionary) algorithm (MOEA) for solving this problem. Coello gave a survey of the MOEA in [13]. Another survey was given in the doctoral thesis of Zitzler [14]. Because of NSGA-II's (Elitist non-dominated sorting based genetic algorithm II) [15] low computational requirements, elitist approach, and parameter-less sharing approach; it was chosen as the algorithm for determination of trade-off between competing performances, i.e. to generate the Pareto front [16,17].

The present paper is organized as follows; Section 2 briefs the basic geometry of rolling bearings. The mathematical model of the problem as a set of objective functions, design parameters and constraints are described in Section 3. Section 4 introduces the concept of the multi-objective optimisation and it discusses whether a deterministic or a stochastic approach is more appropriate for this problem. Section 5 details the application methodology, optimised results and the sensitivity analysis. Section 6 concludes the present work, and is followed by important references. Results obtained are satisfactory, and give a good insight into the trade-offs among the performance measures of rolling bearings. Apart from the numerical significance of the obtained optimal solution, these results can help us in better understanding the parameters behind the effective designing of rolling bearings.

2. Macro-geometries of rolling bearings

Rolling bearings appear to have a simple outer geometry, but their internal geometry can have varying effects on the amount of stresses, deflections and load distributions it can handle. Therefore, the internal geometry has a direct effect on the performance and the life of a bearing. Fig. 1 shows the common nomenclature of a typical rolling bearing.

In the crudest form, the geometry of a bearing can be defined by three *boundary dimensions*, namely, the bore diameter (d), the outer diameter (D) and the bearing width (B_w). These boundary dimensions have been standardised. Parameters that help to define the complete internal geometry of a given rolling bearing (i.e. for a given boundary dimensions) are the ball diameter (D_b), the pitch diameter of the bearing (D_m), the inner and outer raceway curvature coefficients (f_i and f_o), and number of rolling elements (Z).

3. Problem formulation of rolling bearing design

We seek to find out the complete internal geometry (i.e. the ball and pitch diameters, the inner and outer raceway curvature coefficients, and number of rolling elements) of a bearing (as specified by standard bearing *boundary dimensions*), while optimizing its performance characteristics and overall life. Presence of more than one objective makes the problem come into the domain of multi-objective optimisation.

Any constrained multi-optimisation optimisation problem is essentially composed of three components, namely, *design parameters*, *objective functions*, and *constraints* (for defining feasible design parameter space). We discuss in brief, these components of the present problem in following sections.

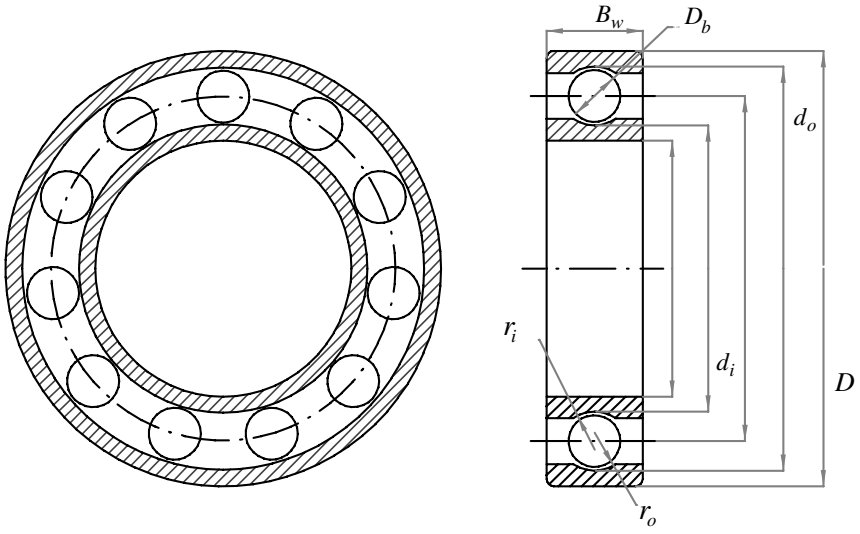

Fig. 1. Macro-geometries of a radial ball bearing.

3.1. Design parameters

The design parameter vector can be written as:

$$X = [D_m, D_b, Z, f_i, f_o, K_{Dmin}, K_{Dmax}, \varepsilon, e, \zeta], \tag{1}$$

where,

$$f_i = r_i/D_b; \quad f_o = r_o/D_b. \tag{2}$$

Parameters that define bearing internal geometries are D_m, D_b, Z, f_i, and f_o (see Appendix A for the nomenclature). Whereas, K_{Dmin}, K_{Dmax}, ε, e, and ζ are part of constraints [11] (refer Section 3.2 and 3.3) and do not directly represent any measurement of the bearing internal geometries. The latter are usually kept constant while designing bearings [7], but for the present case these secondary parameters are also considered as variables. This has been made possible due to the flexibility and the robustness offered by the adopted GA based approach. All angles are measured in radians, dimensions in millimetres – with the exception of the minimum film thickness (H_{min}) that is measured in micrometers, and forces in Newton (N). Assembly angle (ϕ_o) of a bearing (see Fig. 2) also forms an important constraint on the number of rolling elements. Based on the geometrical derivation presented in [11], one could arrive at the following formula for the assembly angle,

$$\phi_o = 2\Pi - 2\cos^{-1}\frac{[\{(D-d)/2 - 3(T/4)\}^2 + \{D/2 - (T/4) - D_b\}^2 - \{d/2 + (T/4)\}^2]}{2\{(D-d)/2 - 3(T/4)\}\{D/2 - (T/4) - D_b\}}, \tag{3}$$

where,

$$T = D - d - 2D_b. \tag{4}$$

3.2. Objective functions

As mentioned earlier, there are three important performance measures of a rolling bearing. These are namely, the dynamic capacity (C_d), the minimum film thickness (H_{min}), and the static capacity (C_s). All of them have to be simultaneously maximized, for getting the best performance of the bearing. These performance parameters are discussed in more detail in the following subsections.

3.2.1. Dynamic capacity (C_d)

Among different objectives for rolling bearings, the dynamic capacity (C_d) is the most important one, as this directly forms the basis for longest *fatigue life* of a bearing. The dynamic capacity, also known as the dynamic

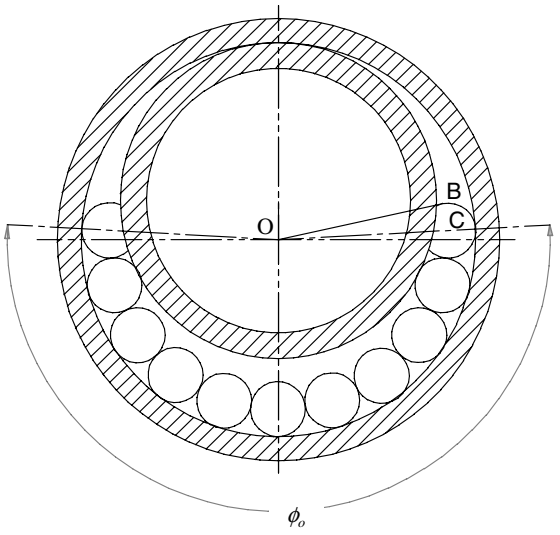

Fig. 2. A rolling bearing showing the assembly angle.

load rating, is defined as "the constant radial load, which a group of apparently identical bearings can endure for a rating life of one million revolutions of the inner ring (for a stationary load and the stationary outer ring)". It is expressed as [7]:

$$C_d = \begin{cases} f_c Z^{2/3} D_b^{1.8} & D_b \leqslant 25.4 \text{ mm} \\ 3.647 f_c Z^{2/3} D_b^{1.4} & D_b > 25.4 \text{ mm} \end{cases} \tag{5}$$

where,

$$f_c = 37.91 \left[1 + \left\{ 1.04 \left(\frac{1-\gamma}{1+\gamma} \right)^{1.72} \left(\frac{f_i(2f_o - 1)}{f_o(2f_i - 1)} \right)^{0.41} \right\}^{10/3} \right]^{-0.3} \left[\frac{\gamma^{0.3}(1-\gamma)^{1.39}}{(1+\gamma)^{1/3}} \right] \left[\frac{2f_i}{2f_i - 1} \right]^{0.41} \tag{6}$$

$$\gamma = D_b \cos\alpha / D_m. \tag{7}$$

Here the factor, γ, is not an independent parameter. For the current discussion, the deep groove ball bearing has been considered, for which the contact angle, α, is zero. Therefore, $\gamma = D_b/D_m$. On careful inspection of Eq. (5), it could be observed that the dynamic capacity depends on (2/3)rd to the power of number of roller and 1.8th to the power the diameter of the ball. Hence, during optimisation, we expect that the maximum possible ball diameter would give us better dynamic capacity. Furthermore, with bigger ball diameter, less number of balls would be accommodated in a given space. The dynamic capacity is derived on the basis of the maximum octahedral shear stress that occurs at the subsurface of the contact zone, between trolling elements and races. Hence, it should be noted that the constraint related to the strength against the shear stress will not appear, explicitly, in constraint section.

3.2.2. Elastohydrodynamic minimum film thickness (H_{min})

Another very important requirement for rolling bearings is the longest wear life. This is directly related to the minimum film thickness (H_{min}) of the lubricant, since it avoids metal-to-metal contact between rolling elements and raceways in rolling bearings. Elastohydrodynamic lubrication (EHL) theory successfully predicts the minimum film thickness [7]. Considering the requirement of low wear, the optimisation problem aims at maximizing the minimum film thickness for a given bearing *boundary dimensions*.

The formula for H_{min} is applicable for the inner and outer raceways separately; therefore, for best results, we maximize the lesser of the two. In Eq. (8), the *ring* can take on values as the *inner* or *outer* ring; see usage in Eq. (9). The complete objective function, for the minimum film thickness, can thus be given as

$$H_{\min,\text{ring}} = 3.63 a_1^{0.49} R_{x,\text{ring}}^{0.466} E_o^{-0.117} Q^{-0.073} \left\{ \frac{\pi n_i D_m \eta_o (1-\gamma^2)}{120} \right\}^{0.68} \left[1 - \exp\left\{ -0.703 \left(\frac{R_{(y,\text{ring})}}{R_{(x,\text{ring})}} \right)^{0.636} \right\} \right] \tag{8}$$

$$H_{\min} = \min(H_{\min,\text{inner}}, H_{\min,\text{outer}}) \tag{9}$$

where i represents number of rows. For the present case, a single-row deep groove rolling bearing has been considered and for this i is equal to 1. Sub-expressions used in the final objective function are listed below

$$Q = \frac{5F_r}{iZ\cos\alpha}, \tag{10}$$

$$R_{(x,\text{inner})} = \frac{D_b}{2(1-\gamma)}, \quad R_{(y,\text{inner})} = \frac{f_i D_b}{2f_i - 1}, \tag{11}$$

$$R_{(x,\text{outer})} = \frac{D_b}{2(1+\gamma)}, \quad R_{(y,\text{outer})} = \frac{f_o D_b}{2f_o - 1}. \tag{12}$$

It should be noted that the nature of Eqs. (8) and (10) is approximate and they should be used with due care. However, a complete load distribution analysis (i.e. finding the maximum load, Q) based on the elastohydrodynamic lubrication (EHL) integrated approach (i.e. simultaneously obtaining H_{min}) is computationally very expensive, with the difficulty of inherent convergence problem [7], and not to mention that it is for a single solution. The implementation of this analysis, with optimum design, would be very difficult and infeasible in terms of the computation time, since it would require such analysis of bearing to be performed more than

hundred thousand times (as in the present case). One should also note that these Eqs. (8) and (10) give conservative estimates of the elastohydrodynamic minimum film thickness and the maximum load.

3.2.3. Static capacity (C_s)

The basic load rating (C_s) (or the static capacity) of a rolling bearing is defined as "that load applied to a non-rotating bearing that will result in the permanent deformation occurring at the position of the maximum loaded rolling element". The static capacity is defined for both the inner as well as the outer raceway. The objective function takes the minimum of both values and maximizes that. This approach is similar to the one employed for $H_{\min}$.

$$C_{s,\text{inner}} = \frac{23.8ZiD_b^2(a_i^* b_i^*)^3 \cos\alpha}{\left(4 - \frac{1}{f_i} + \frac{2\gamma}{1-\gamma}\right)^2}; \quad C_{s,\text{outer}} = \frac{23.8ZiD_b^2(a_o^* b_o^*)^3 \cos\alpha}{\left(4 - \frac{1}{f_o} - \frac{2\gamma}{1+\gamma}\right)^2} \tag{13}$$

$$C_s = \min(C_{s,\text{inner}}, C_{s,\text{outer}}) \tag{14}$$

The basis of the derivation of the static capacity is the maximum contact stress, which occurs between the rolling element and races. Hence, the constraint related to the contact stress will not reflect in the constraint, explicitly.

3.3. Constraints

Constraints reduce the parameter space to the *feasible* parameter space. This section summarises the nine problem constraints. Apart from geometrical constraints, we also maintain an intuitive constraint on the number of balls in a given bearing. The first constraint, for the maximum allowance on the assembly angle is [11]

$$\frac{\phi_0}{2\sin^{-1}(D_b/D_m)} - Z + 1 \geqslant 0. \tag{15}$$

This establishes convenience in the bearing assembly and numbers of balls that can be inserted in between the inner and outer raceways. The assembly angle (ϕ_o) is found by Eq. (3), which employs important design variables.

The ball diameter gets an upper and lower bound, through following constraints

$$2D_b - K_{D\min}(D-d) \geqslant 0, \tag{16}$$

$$K_{D\max}(D-d) - 2D_b \geqslant 0. \tag{17}$$

Furthermore, an additional constraint, based on the bearing width, which limits the maximum allowable diameter of the ball, is

$$\zeta B_w - D_b \leqslant 0. \tag{18}$$

To guarantee the running mobility of bearings, we must insure that the difference between the pitch diameter and the average diameter in a bearing should be less than a certain value. The inner ring thickness must also be more than the outer ring thickness, therefore,

$$D_m - 0.5(D+d) \geqslant 0 \tag{19}$$

$$(0.5+e)(D+d) - D_m \geqslant 0. \tag{20}$$

The thickness of a bearing ring, at the outer raceway bottom, should not be less than εD, where ε is a parameter obtained from the simple strength consideration of the outer ring. The constraint condition is then

$$0.5(D - D_m - D_b) - \varepsilon D_b \geqslant 0. \tag{21}$$

The groove curvature radii of the inner and outer raceways of a bearing should not be less than 0.515 D_b [7], this ensures that the rolling element rolls freely on raceways without any interference. Therefore,

$$f_i \geqslant 0.515, \tag{22}$$

$$f_o \geqslant 0.515. \tag{23}$$

4. Multi-objective optimization

The optimisation is a key word in most of engineering applications. An engineering design optimisation problem is generally composed of multiple objectives, associated with a constrained parameter space, thereby getting the name as (constraint) multi-objective optimisation. Formally, the multi-objective optimisation refers to the solution of problems with two or more objective functions, which are normally in conflict with each other. Such *trade-off fronts* are also termed as *Pareto optimal fronts*, named after Vilfredo Pareto who stated this concept in 1896 [16–18]. The problem of multi-objective optimisation can be represented mathematically as

$$\text{optimize } \mathbf{f}(\mathrm{p}) = \begin{bmatrix} f_1(p) \\ f_2(p) \\ \vdots \\ f_n(p) \end{bmatrix} \text{ subjected to } \mathbf{c}(\mathbf{p}) \geqslant 0; n \geqslant 2. \tag{24}$$

Here, **p** represents the *parameter vector*, **f(p)** represents the *objective vector* and **c(p)** represents the *constraints vector*. In remainder of this paper, without loss of generality, all the optimisation would be of minimization type, since one can always convert a maximization into minimization by multiplying it with a (-1). The concept of *Pareto optimality* can also be well understood graphically, consider Fig. 3 that uses 2-dimensional planes to represent a multi-dimensional co-ordinate space. Here, the *parameter* space is represented by $\mathscr{P}$ and the *objective* space is represented by $\mathscr{F}$. The parameter space is m-dimensional, and the objective space is n-dimensional. It gives

$$F = \{\mathbf{f}|\mathbf{f} = \mathbf{f}(\mathbf{p}) \wedge \mathbf{p} \in P\}, \tag{25}$$

$$P = \{\mathbf{p}|\mathbf{c}(\mathbf{p}) \geqslant 0\}. \tag{26}$$

This mapping could either be linear or nonlinear in nature. For the present problem of optimisation in rolling bearings, it happens to be nonlinear in nature. It goes without saying, that nonlinear mapping is harder to handle.

In the multi-objective optimisation, a solution vector $\mathbf{x} = [x_1, x_2, \ldots x_n]$ is considered more optimal than vector $\mathbf{y} = [y_1, y_2, \ldots y_n]$ if **x** *dominates* **y** as in Eq. (27). This implies that all elements in **x** are smaller than or equal to corresponding elements in **y**, and at least one of them in **x** is *strictly* smaller than its counterpart in **y**. The set of *non-dominated* points make up the *Pareto optimal front*. The region marked as $\partial F^{\prec}$ in Fig. 3 represents *Pareto optimal front* in the objective space.

$$\mathbf{x} \prec \mathbf{y} : \iff \underset{i\in\{1,2,3\ldots,n\}}{\forall} (x_i \leqslant y_i) \wedge \underset{i\in\{1,2,3\ldots,n\}}{\exists} (x_i < y_i). \tag{27}$$

Multi-objective algorithms can be sub-divided into two primary categories – deterministic or stochastic algorithms. The choice between these two has to take into account a number of factors – problem complexity

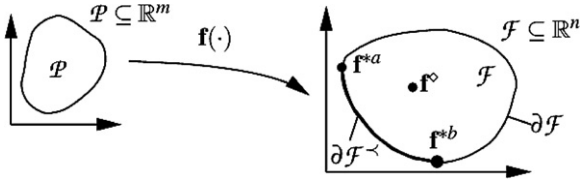

Fig. 3. Mapping of the parameter space $\mathscr{P}$ to the objective space $\mathscr{F}$. ($\mathbf{f}^{\langle\rangle}$ represents a random point in the objective space. And, $\partial\Phi^{\prec}$ marks the Pareto optimal front, with $\mathbf{f}^{*a}$ and $\mathbf{f}^{*b}$ as the end points of the front.)

(number of objectives and parameters), parameter space (as defined by constraints) and the resources available (time and space). The design of a rolling bearing is a nonlinear multi-objective optimisation problem with moderate complexity – three objective functions, nine parameters and nine inequality constraints (refer to Section 3). Deterministic multi-objective optimisation strategies are notorious for getting stuck at local minima and explode in complexity with the increase in number of parameters. Further, each run of the deterministic algorithm can provide only single point on the Pareto optimal front. On the other hand, stochastic algorithms easily dodge local minima, handle parameters more efficiently and a single run of the evolutionary algorithm can provide numerous non-dominated solution points, thus giving us a close approximation of Pareto optimal front. In the light of all these factors the evolutionary algorithm for the multi-objective optimisation was chosen for application to the current problem.

Over the past decade, a number of multi-objective evolutionary algorithms (MOEAs) have been suggested. The primary reason for this is their ability to find multiple Pareto-optimal solutions in a single run. For problems with a multi-objective formulation, it is not possible to have a single solution, which simultaneously optimizes all objectives. In such cases, an algorithm that gives a large number of alternative solutions lying on or near the Pareto-optimal front is of great practical value. With the growing complexity of engineering problems, popularity of evolutionary algorithms has been on a rise. A good survey and comparison of recent evolutionary multi-objective optimisation algorithm can be gathered from [13,14,16–18]. More recently, strength-Pareto EA (SPEA), Pareto-archived evolution strategy (PAES) and NSGA II have gained tremendous popularity for their superior performances. Out of these NSGA II stands out for its fast non-dominated sorting approach, elitism approach and its overall capability to maintain a better solution spread. Thus being a motivation for its use in the design of rolling bearings as presented in this paper. The finer details of this algorithm can be gathered from [15].

5. Application and results

The work on the design optimisation of rolling bearings is a very active area of research. Some contribution on the design of rolling bearings was made by earlier work of Chakraborty et al. [10] and Rao and Tiwari [11], where GA was used to optimize dynamic capacity for rolling bearings. Results in [10,11] were found to be as much as 1.5 times better than those given in standard bearing catalogue [19]. Primary difference between previous works and that presented in this paper is the inclusion of multiple objectives for the simultaneous optimisation.

5.1. NSGA II implementation and application

NSGA II implementation written by KanGAL, IIT Kanpur [20] was used as the optimisation engine. A wrapper module was written in the C computer language over this optimisation engine, to handle the multi-objective optimisation problem for rolling bearings. The module allows user to specify boundary dimensions of the bearing, choose objectives of interest, vary parametric ranges and specify sensitive GA parameters. Real coded chromosomes were used to encode nine design parameters, which are defined in Section 3.1. Problem constraints were incorporated using the standard constraint handling technique [17]. Problem parameters were given the strict upper and lower bounds (Table 1) to reduce the solution space. Operating conditions are listed in Table 2, these are same as in [12].

As discussed in Section 3.2, there are three objectives for optimisation – (1) the dynamic capacity C_d, (2) the static capacity C_s and (3) the elastohydrodynamic minimum film thickness H_{min}. An exhaustive treatment was given to the optimisation problem by choosing all possible combinations of aforementioned objectives. Each of these combinations was optimised over a broad set of standard bearing boundary dimensions, i.e. the outer diameter, D, the bore diameter, d and the bearing width B_w. Thus following optimisation runs were made:

- Single objective optimisations: C_d (Table 3), H_{min} (Table 4) and C_s (Table 5).
- Dual objective optimisations: C_d–C_s (Table 6), C_d–H_{min} (Table 7) and C_s–H_{min} (Table 8).
- Multi-objective optimisation: C_d–C_s–H_{min} (Table 9).

Table 1
Parametric bounds

$D_m \sim \{0.5(D+d), 0.6(D+d)\}$
$D_b \sim \{0.15(D-d), 0.45(D-d)\}$
$Z \sim (4, 50)$
$f_i \sim (0.515, 0.6)$
$f_o \sim (0.515, 0.6)$
$K_{Dmin} \sim (0.4, 0.5)$
$K_{Dmax} \sim (0.6, 0.7)$
$\varepsilon \sim (0.3, 0.4)$
$E \sim (0.02, 0.10)$
$\zeta \sim (0.6, 0.85)$

Table 2
Operating conditions

$\alpha_1 = 1e-08$
$\eta_o = 0.02$
$n_i = 5000$
$E_o = 2.25e+11$
$F_r = 15000$

A step-by-step procedure for solving the given optimisation problem is illustrated in Fig. 4. The figure assumes understanding of the basic GA terminology. Readers are encouraged to gather more details about NSGA II from [15]. The population size, the generation count, the crossover and mutation probabilities were determined after multiple runs of the algorithm with the aim of obtaining *best* solutions. *Best* here implies the maximum spread of solution points and high values of all the objectives simultaneously. The *best* results were decided from a solution set of 20 runs with varying mutation and crossover probabilities, where each GA run used a random seed for generation of the initial population.

The population size was set as 4500 for all the runs, and the convergence was achieved by the end of 50th generation for all combinations of the objectives (some combinations converged before 50th generation, but none after). The value of crossover probability used ranged from 0.7 to 0.85 and the value mutation probability used ranged from 0.15 to 0.2. Although there was no significant impact of variation in these two GA parameters on the obtained solutions, the number of GA generations required for achieving convergence increased for values of crossover and mutation probabilities outside this range. The crossover distribution and mutation distribution indices, introduced from the use of real coded chromosomes, were found to be the most influential NSGA II parameters in the current context. They were assigned values in order to achieve the maximum spread of solution points. Data from multiple runs favoured the crossover distribution index of 20, and the mutation distribution index of 10. The lower values of these distribution indices usually gave a wider spread to solutions and hence a better approximation of the Pareto-optimal front.

Tables 3–5 give the best optimisation results obtained for the dynamic capacity (C_d), the minimum film thickness (H_{min}) and the static capacity (C_s), respectively. Each of these optimisations is a single objective optimisation. Table 3 also compares dynamic capacities of optimized bearings with the existing standard [19]. In order to compare the increase in the fatigue life of the designed bearings using GAs against the standard values, the relation shown in Eq. (28) has been used. The subscripts d_new and d_std represent the new values computed using GA and those currently available in standards, respectively,

$$\lambda = \left(\frac{C_{d\_new}}{C_{d\_std}}\right)^3. \tag{28}$$

Tables 6–8 show the best results for dual objective optimizations, i.e. dynamic capacity – minimum film thickness, dynamic capacity – static capacity and static capacity – minimum film thickness, respectively. These optimisations are actually the ones that exploited the capability of multi-objective optimisations. The trade-off front approximation, obtained after every few generation count of NSGA II, was recorded to keep track

Table 3
Optimisation of the dynamic capacity C_d and its comparison with standard catalogue values

Boundary dimensions (mm)			Design parameters					Converged constraint constants						Dynamic capacity (N)		
D	d	B_w	D_m	D_b	Z	r_i	r_o	K_{Dmin}	K_{Dmax}	E	e	ζ	ϕ_o (rads)	C_{d_new}	C_{d_std} [19]	λ
30	10	9	20.05977	6.2111	7	3.1987	3.199	0.4298	0.6342	0.300063	0.0345	0.7143	3.7784	6029.54	3580	4.77753
35	15	11	25.00078	6.2494	8	3.2184	3.2184	0.405	0.6734	0.300018	0.0746	0.8413	3.6125	7057.92	5870	1.73826
47	20	14	33.50005	8.4372	8	4.3452	4.3452	0.4184	0.6292	0.3	0.0202	0.6394	3.6174	12098.9	9430	2.11202
62	30	16	46.00001	9.9996	9	5.1498	5.1498	0.4438	0.6579	0.300006	0.0319	0.6777	3.5329	18111.9	14900	1.79611
80	40	18	60.00047	12.499	9	6.4368	6.4368	0.4324	0.6455	0.300005	0.0896	0.7722	3.512	27138.7	22500	1.75477
90	50	20	70.73144	12.038	11	6.1996	6.1996	0.4028	0.693	0.300008	0.035	0.6809	3.4205	28997	26900	1.25258
110	60	22	85.00224	15.623	10	8.0459	8.0458	0.4156	0.6278	0.300027	0.02	0.7992	3.4581	43607.1	40300	1.26694
125	70	24	98.22011	16.73	11	8.6162	8.6162	0.4549	0.6698	0.300085	0.0955	0.7695	3.4235	52443.3	47600	1.33736
140	80	26	110.0008	18.749	11	9.6557	9.6557	0.4003	0.6668	0.300001	0.0261	0.8358	3.4302	64376.2	55600	1.55222
160	90	30	125.7171	21.423	11	11.033	11.033	0.4159	0.651	0.300043	0.0223	0.751	3.4251	81843.3	73900	1.35836

Table 4
Optimisation of the elastohydrodynamic minimum film thickness H_{min}

Boundary dimensions (mm)			Design parameters					Converged constraint constants						Elastohydrodynamic minimum film thickness (μm)
D	d	B_w	D_m	D_b	Z	r_i	r_o	K_{Dmin}	K_{Dmax}	E	e	ζ	ϕ_o (rads)	H_{min}
30	10	9	22.546	4.6579	9	2.3988	2.407	0.4068	0.6275	0.300024	0.0794	0.6386	3. 401321	0.2193
35	15	11	26.919	5.0507	10	2.6012	2.6025	0.4017	0.6578	0.300006	0.0411	0. 6116	3.40058	0.2631
47	20	14	36.143	6.7831	10	3.4933	3.4934	0.4049	0.6561	0.300128	0.0574	0.6378	3.398662	0.3688
62	30	16	47.539	9.0381	10	4.6547	4.6551	0.4016	0.605	0.30001	0.0265	0.6531	3.443431	0.5069
80	40	18	61.301	11.686	10	6.0185	6.0185	0.4036	0.6606	0.300026	0.0525	0.6537	3.454562	0.6789
90	50	20	70.737	12.039	11	6.2	6.4149	0.4566	0.6038	0.300002	0.0822	0.7814	3.420553	0.777
110	60	22	86.497	14.689	11	7.5651	7.7261	0.427	0.666	0.300005	0.0478	0.8015	3.413632	0.9777
125	70	24	98.236	16.727	11	8.6145	8.8275	0.4701	0.6452	0.300004	0.0431	0.7894	3.423332	1.1322
140	80	26	110	18.749	11	9.6557	9.6557	0.4003	0.6668	0.300001	0.0261	0.8358	3.43022	1.2894
160	90	30	125.72	21.424	11	11.033	11.034	0.439	0.6744	0.300005	0.0204	0.8343	3.425148	1.5025

Table 5
Optimisation of the static capacity C_s

Boundary dimensions (mm)			Design parameters					Converged constraint constants						Static capacity (N)
D	d	B_w	D_m	D_b	Z	r_i	r_o	K_{Dmin}	K_{Dmax}	E	e	ζ	ϕ_o (rads)	C_s
30	10	9	20.06	6.2111	7	3.1987	3.199	0.4298	0.6342	0.300063	0.0345	0.7143	3.7784	3672.966
35	15	11	25.001	6.249	8	3.2182	3.2188	0.4008	0.6475	0.300001	0.0464	0.6004	3.6124	4766.734
47	20	14	33.5	8.4372	8	4.3452	4.3452	0.4184	0.6292	0.3	0.0208	0.6036	3.6174	8658.353
62	30	16	46.001	9.9996	9	5.1498	5.15	0.4038	0.6397	0.300003	0.07	0.7053	3.5329	14562.01
80	40	18	61.293	11.689	10	6.0201	6.0201	0.4101	0.6401	0.30004	0.0864	0.7737	3.4548	23158.69
90	50	20	70.737	12.039	11	6.2	6.2126	0.4002	0.6296	0.300011	0.0216	0.6889	3.4206	27970.82
110	60	22	85.007	15.619	10	8.0439	8.0452	0.4039	0.6334	0.300013	0.0593	0.7764	3.4579	41839.28
125	70	24	98.228	16.73	11	8.6161	8.6163	0.4226	0.6309	0.300065	0.055	0.7558	3.4235	54007.23
140	80	26	110	18.748	11	9.6551	9.809	0.4815	0.6691	0.300016	0.0866	0.7974	3.4302	67805.37
160	90	30	125.72	21.424	11	11.033	11.303	0.4212	0.6997	0.300053	0.0953	0.8455	3.4252	88548.01

Table 6
Simultaneous optimisation of the dynamic capacity C_d and the static capacity C_s

Boundary dimensions (mm)			Design parameters					Converged constraint constants						Dynamic and static capacity	
D	d	B_w	D_m	D_b	Z	r_i	r_o	K_{Dmin}	K_{Dmax}	E	e	ζ	ϕ_o (rads)	C_d	C_s
30	10	9	20.06	6.2111	7	3.1987	3.199	0.4298	0.6342	0.300063	0.0345	0.7143	3.778398	6029.5	3672.97
35	15	11	25.001	6.2493	8	3.2184	3.2184	0.4019	0.6771	0.300004	0.0584	0.729	3.612473	7057.9	4766.73
47	20	14	33.5	8.4372	8	4.3452	4.3452	0.485	0.6739	0.300015	0.0208	0.6036	3.617353	12099	8658.35
62	30	16	46.001	9.9996	9	5.1498	5.15	0.4038	0.6397	0.300003	0.07	0.7053	3.532938	18111	14562
80	40	18	60	12.499	9	6.4368	6.4368	0.4324	0.6455	0.300005	0.0896	0.7722	3.512029	27139	23115.2
90	50	20	70.738	12.038	11	6.1995	6.1995	0.4957	0.6943	0.30004	0.0818	0.7835	3.420498	28997	27967.1
110	60	22	85.007	15.619	10	8.0438	8.0443	0.4644	0.6975	0.300019	0.0825	0.8495	3.457942	43586	41838.6
125	70	24	98.22	16.73	11	8.6162	8.6162	0.4549	0.6698	0.300085	0.0955	0.7695	3.423463	52443	54006.2
140	80	26	110	18.748	11	9.6551	9.6551	0.4043	0.6638	0.300007	0.0578	0.7516	3.430182	64372	67804.2
160	90	30	125.72	21.423	11.562	11.033	11.033	0.4774	0.7	0.300063	0.0998	0.8169	3.42512	81841	88539.7

Table 7
Simultaneous optimisation of the dynamic capacity C_d and the elastohydrodynamic minimum film thickness H_{min}

Boundary dimensions (mm)			Design parameters					Converged constraint constants						Dynamic capacity and minimum film thickness	
D	d	B_w	D_m	D_b	Z	r_i	r_o	K_{Dmin}	K_{Dmax}	E	e	ζ	ϕ_o (rads)	C_d	H_{min}
30	10	9	20.561	5.899	7	3.038	3.0383	0.4172	0.6161	0.300019	0.0342	0.7886	3.6945	5635.2	0.20873
35	15	11	25.495	5.9403	8	3.0592	3.0593	0.4752	0.6125	0.300008	0.0202	0.6601	3.5549	6510.9	0.25843
47	20	14	34.25	7.967	8	4.103	4.103	0.4013	0.6176	0.300047	0.0214	0.6421	3.5518	11045	0.36231
62	30	16	46.156	9.902	9	5.0996	5.0996	0.4014	0.6192	0.300001	0.0268	0.6378	3.5236	17812	0.50366
80	40	18	60.052	12.467	9	6.4207	6.4233	0.4007	0.6353	0.300003	0.0482	0.7245	3.5098	27007	0.67476
90	50	20	70.741	12.036	11	6.1988	6.1989	0.4615	0.6361	0.300028	0.0262	0.7415	3.4204	28987	0.77698
110	60	22	85.002	15.623	10	8.0459	8.0458	0.4156	0.6278	0.300027	0.02	0.7992	3.4581	41487	0.97771
125	70	24	98.234	16.727	11	8.6143	8.6149	0.4589	0.6994	0.300019	0.0386	0.7472	3.4233	52414	1.13221
140	80	26	110	18.749	11	9.6557	9.6557	0.4003	0.6668	0.300001	0.0261	0.8358	3.4302	64376	1.28936
160	90	30	125.72	21.423	11	11.033	11.033	0.4983	0.6329	0.300019	0.0205	0.7768	3.4251	81836	1.50254

Table 8
Simultaneous optimisation of the static capacity C_s and the elastohydrodynamic minimum film thickness H_{min}

Boundary dimensions (mm)			Design parameters					Converged constraint constants						Static capacity and minimum film thickness	
D	d	B_w	D_m	D_b	Z	r_i	r_o	K_{Dmin}	K_{Dmax}	E	e	ζ	ϕ_o (rads)	C_s	H_{min}
30	10	9	21.382	5.3862	8	2.774	2.774	0.4001	0.6001	0.300007	0.0414	0.604	3.5662	3528.2	0.2151
35	15	11	25.176	6.139	8	3.162	3.165	0.4028	0.6325	0.300012	0.0786	0.7453	3.5916	4651.7	0.2575
47	20	14	33.795	8.2529	8	4.25	4.266	0.4032	0.6332	0.3	0.0222	0.6178	3.5913	8401	0.36097
62	30	16	46.133	9.9166	9	5.107	5.108	0.4127	0.6552	0.300002	0.02	0.6662	3.525	14382	0.50363
80	40	18	61.297	11.689	10	6.02	6.031	0.4024	0.673	0.300005	0.0574	0.7441	3.4547	23157	0.67894
90	50	20	70.737	12.039	11	6.2	6.207	0.434	0.6346	0.300002	0.0267	0.6407	3.4205	27970	0.777
110	60	22	86.495	14.69	11	7.565	7.577	0.4342	0.6985	0.300007	0.0667	0.7816	3.4136	41670	0.97772
125	70	24	98.236	16.727	11	8.615	8.679	0.4169	0.6537	0.300009	0.0901	0.7973	3.4233	53992	1.13224
140	80	26	110	18.747	11	9.655	9.943	0.4	0.6761	0.300006	0.023	0.7802	3.4302	67802	1.28935
160	90	30	125.72	21.422	11	11.03	11.16	0.4354	0.6384	0.300003	0.0308	0.7384	3.4251	88548	1.50251

of the progress and determine the convergence of the trade-off to the Pareto-optimal front. Every dual objective optimisation gave approximately 50–100 trade-off solution points. Entries in the table list only the *knee* point value (i.e. solutions of the trade-off front where a small improvement in one objective would lead to a large deterioration in at least one other objective) of the approximate Pareto optimal front, which were finally obtained. Figs. 5–14 show the Pareto optimal front obtained for a few of the optimisation runs.

Table 9 shows the best results for the multi-objective optimisation of all three objectives. GA parameters used were the same as in the case of dual objective optimisation. Each optimisation run produced a set of solution triplets (C_d–C_s–H_{min}), and the *knee* points have been listed in Table 9. The solution set did not represent a three-dimensional trade-off front since the dynamic and static capacities optimised simultaneously. This is due to the fact that the dynamic and static capacities are defined based on stresses (i.e. the octahedral shear and contact normal stresses, respectively). This fact is supported by results shown in Figs. 5, 9 and 12. In contrast to the behaviour between the static and dynamic capacities, the minimum film thickness was found to be a conflicting objective against both the dynamic capacity as well as the static capacity. Figs. 6,7,10,11,13 and 14 show these results.

Maximum running time of the algorithm (for a single bearing configuration) was 178 s on a Pentium4 HT 3.0 GHz machine with 512 MB of RAM on a Fedora Core 4 Linux distribution. This maximum time was reached for the case when all three objectives were optimised simultaneously with a population size of 4500. Single objective optimisation took an average run time of 86 s, and dual-objective optimisation took an average run time of 130 s (average run time was computed across the combinations of objective functions).

Table 9
Simultaneous optimisation of the dynamic capacity C_d, the elastohydrodynamic minimum film thickness H_{min} and the static capacity C_s

Boundary dimensions (mm)			Design parameters					Converged constraint constants						Dynamic capacity, minimum film thickness and static capacity		
D	d	B_w	D_m	D_b	Z	r_i	r_o	K_{Dmin}	K_{Dmax}	E	e	ζ	ϕ_o (rads)	C_d	H_{min}	C_s
30	10	9	20.702	5.81	7	2.9919	2.9974	0.4046	0.6057	0.300011	0.057	0.693	3.6713	5511.5	0.2096	3401.91
35	15	11	25.37	6.017	8	3.099	3.1069	0.4072	0.6461	0.30002	0.0236	0.601	3.569	6630.8	0.2581	4522.08
47	20	14	34.131	8.042	8	4.1418	4.1419	0.4005	0.6196	0.300002	0.024	0.604	3.5621	11215	0.362	8103.52
62	30	16	46.196	9.876	9	5.0861	5.1361	0.4011	0.6322	0.300027	0.054	0.656	3.5211	17522	0.5037	14292.7
80	40	18	0.0338	12.48	9	6.4265	6.4273	0.4	0.655	0.300011	0.0234	0.736	3.5106	27060	0.6748	23059.3
90	50	20	70.739	12.04	11	6.1991	6.1991	0.4089	0.6157	0.300046	0.0306	0.631	3.4205	28993	0.777	27963.9
110	60	22	85.001	15.62	10	8.046	8.1492	0.4027	0.6677	0.300039	0.0591	0.762	3.4581	42691	0.9763	41854.1
125	70	24	98.229	16.73	11	8.6166	8.6167	0.4951	0.6362	0.30001	0.0802	0.835	3.4235	52447	1.1323	54012
140	80	26	110	18.75	11	9.6557	9.656	0.4014	0.645	0.300007	0.0204	0.748	3.4302	64372	1.2894	67806.5
160	90	30	125.72	21.43	11	11.034	11.034	0.4517	0.6511	0.300001	0.0462	0.825	3.4252	81858	1.5026	88558

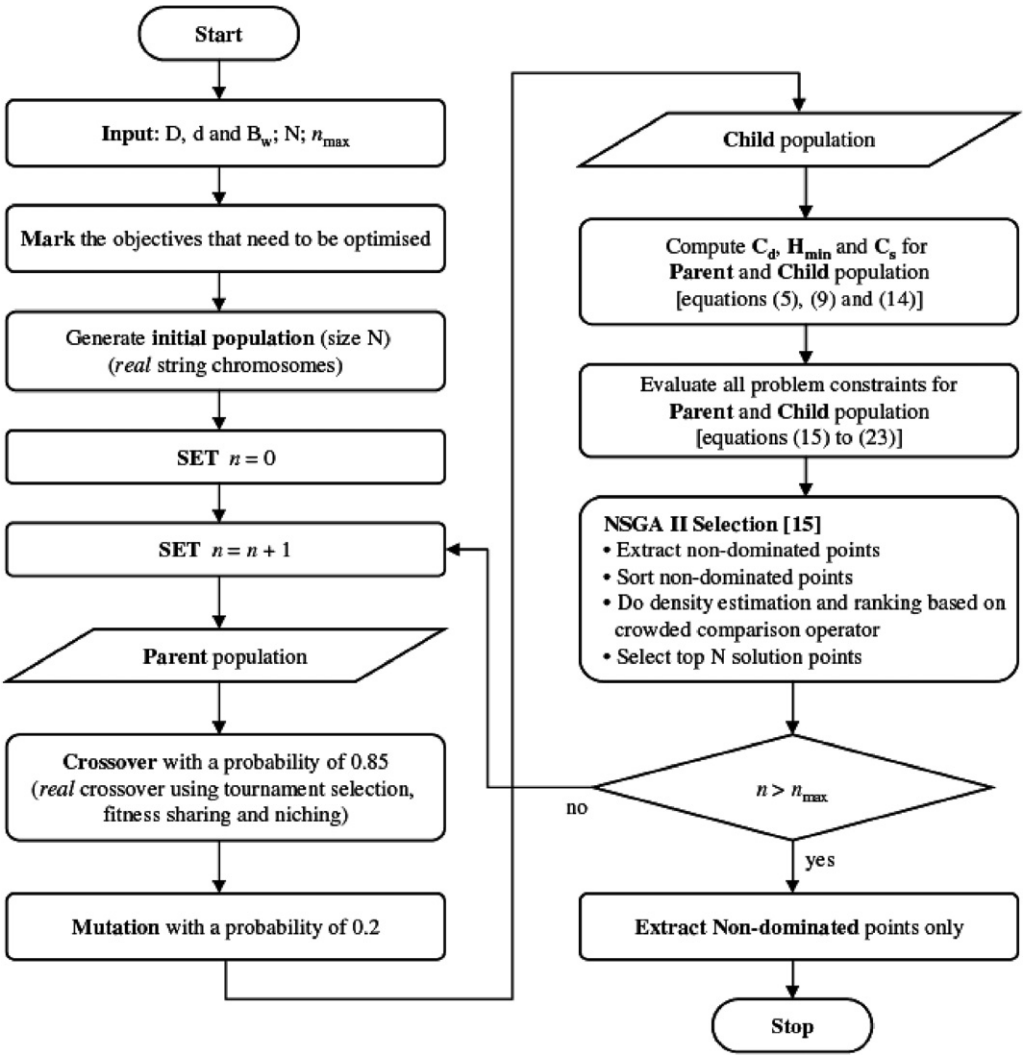

Fig. 4. Application of NSGA II to the multi-objective optimisation of rolling element bearings. For the results presented in this paper, population size (N) was set as 4500 and number of generations (n_{max}) as 50.

In general, the time taken was found to be directly proportional to the number of generations, which is not uncommon for a GA.

As an example of the optimised bearing design obtained, Fig. 8 shows the axial and radial cross-sectional views for a typical bearing (boundary dimensions $D = 30$ mm, $d = 10$ mm and $B_w = 9$ mm) after dynamic capacity optimisation using the approach discussed in this paper.

5.2. Parametric sensitivity analysis

At the time of manufacturing, it is not uncommon to see 0.5–1% deviation in the design parameter values. To better evaluate a bearing design, it is important to observe the sensitivity in the values of the obtained performance measures with respect to such parametric variations. This section attempts to answer this concern, of designs obtained by using the approach discussed in this paper.

Out of all parameters detailed in Section 3.1, the ones that influence the performance measures and can suffer from manufacture tolerances are D_m, D_b, f_i and f_o. Therefore, we will study the performance impact of varying these parameters by a maximum of 1% around a given nominal optimised solution point. Variation

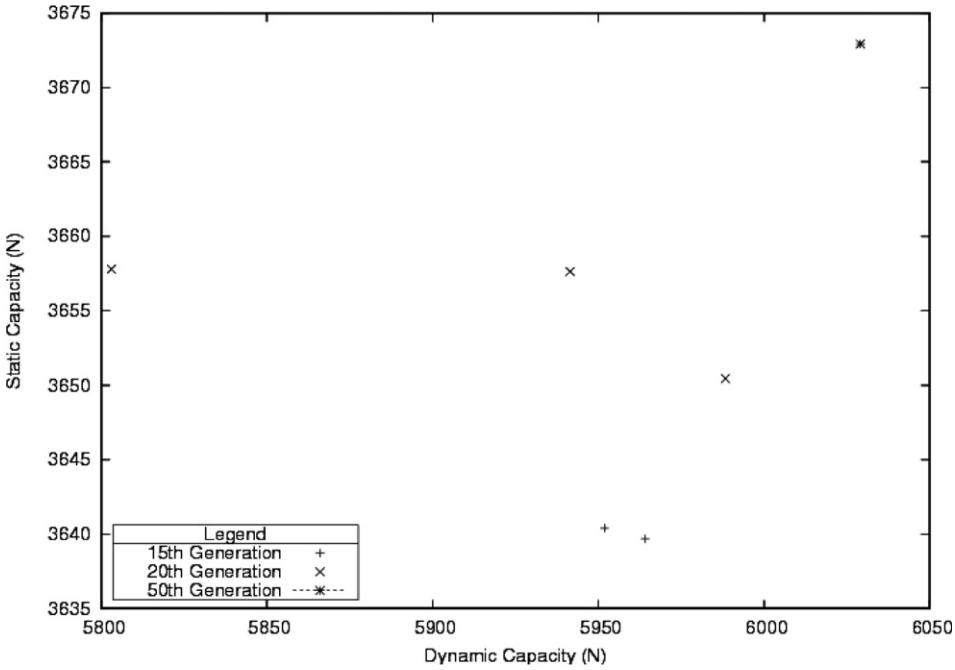

Fig. 5. Graph for simultaneous optimisation of static capacity and dynamic capacity. Bearing configuration: $D = 30$ mm, $d = 10$ mm, and $B_w = 9$ mm. Evidently there is little or no trade-off between these two objectives. By the 50th generation the algorithm converges to only one simultaneously optimal solution point.

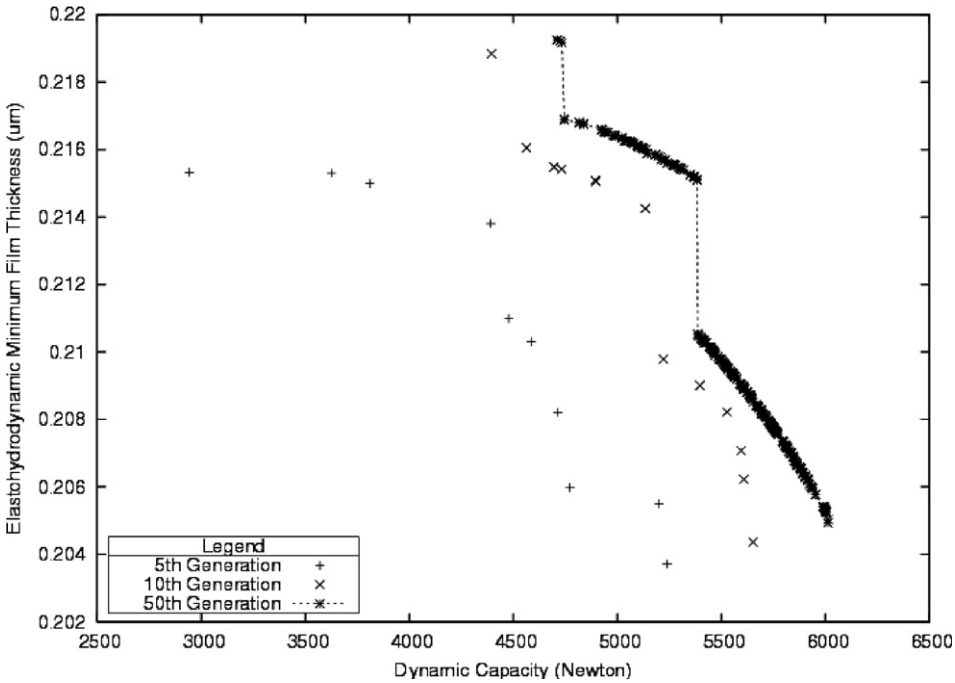

Fig. 6. Graph for simultaneous optimisation of dynamic capacity and minimum film thickness. Bearing configuration: $D = 30$ mm, $d = 10$ mm, and $B_w = 9$ mm. A definite trade-off is easy to make out from this plot. By the end of 50th generation the trade-off front given by the algorithm converges. The vertical drops indicate absence of Pareto optimal points in the intermediate region.

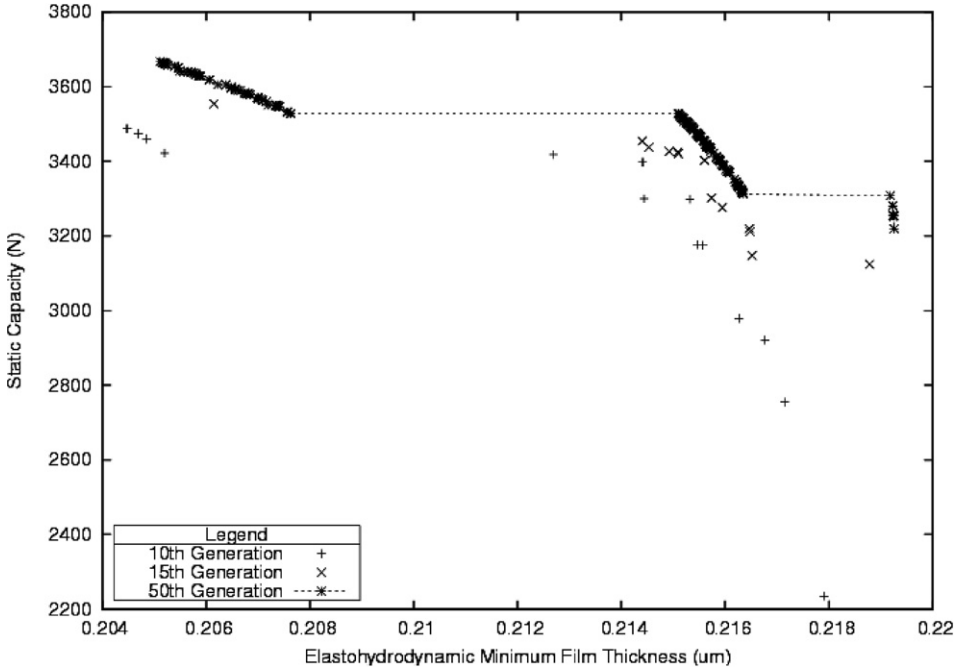

Fig. 7. Graph for simultaneous optimisation of minimum film thickness and static capacity. Bearing configuration: $D = 30$ mm, $d = 10$ mm, and $B_w = 9$ mm. Here again a definite trade-off is observed. By the end of 50th generation the trade-off front given by the algorithm converges. The horizontal sweeps indicate absence of Pareto optimal points in the intermediate region.

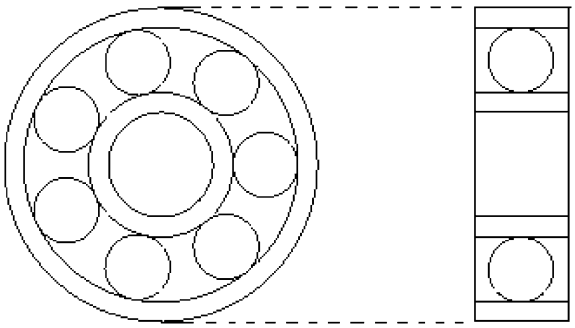

Fig. 8. Radial and axial cross-sectional view of a rolling bearing designed by the algorithm, finer dimension like f_i and f_o are not shown here. This bearing has $D_m = 20.0597$ mm, $D_b = 6.211$ mm, $Z = 7$ and Dynamic capacity $C_d = 6954.463$ N.

in parameters has been done, by generating random points within a 1% neighbourhood of the representative point. A uniform distribution was used to generate these random points. For example, when doing the sensitivity analysis with respect to the ball diameter, D_b is varied by 1% around its original value and all other parameters are kept fixed. We will demonstrate the sensitivity of all three objectives with respect to each of these parameters, separately and collectively.

A quantitative approach has been taken for the sensitivity analysis, therefore we have to compute sensitivity of performance measures around a given solution point. As a representative optimised solution point, we use the result for bearing configuration: ($D = 30$, $d = 10$, $B_w = 9$) from Table 9. For the sake of brevity; results are discussed for this one representative solution point. Similar trends were observed for other solution points as well.

- Ball diameter (D_b): Performance measures vary by less than 1% for changes in the ball diameter (Fig. 15). H_{min}, in specific, has a negligible change in its value. Therefore, the present design is acceptable when tolerances in design parameters do not exceed this limit at the time of manufacturing.

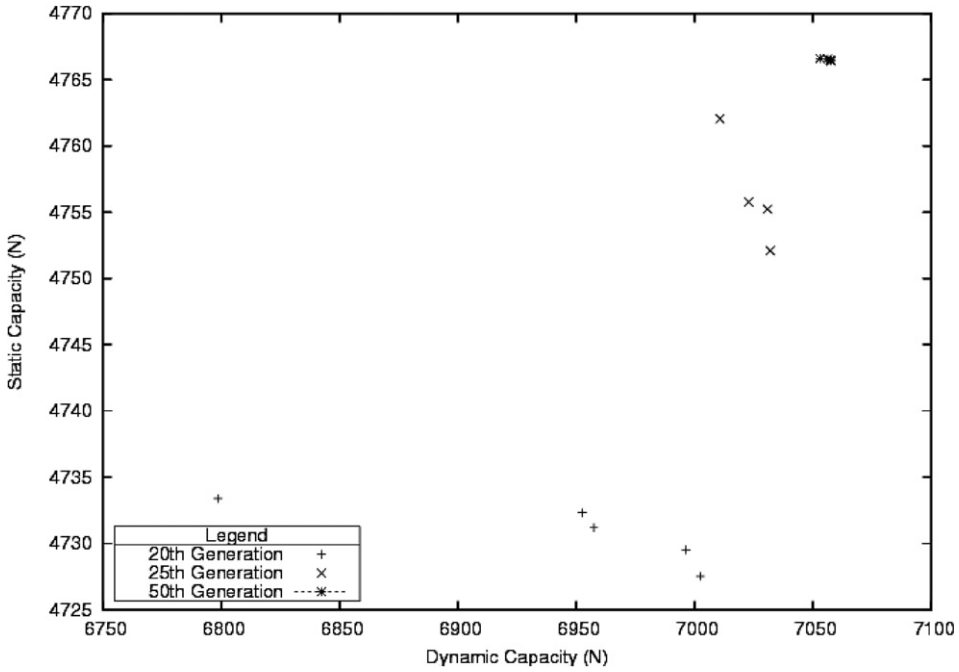

Fig. 9. Graph for simultaneous optimisation of static capacity and dynamic capacity. Bearing configuration: $D = 35$ mm, $d = 15$ mm, and $B_w = 11$ mm.

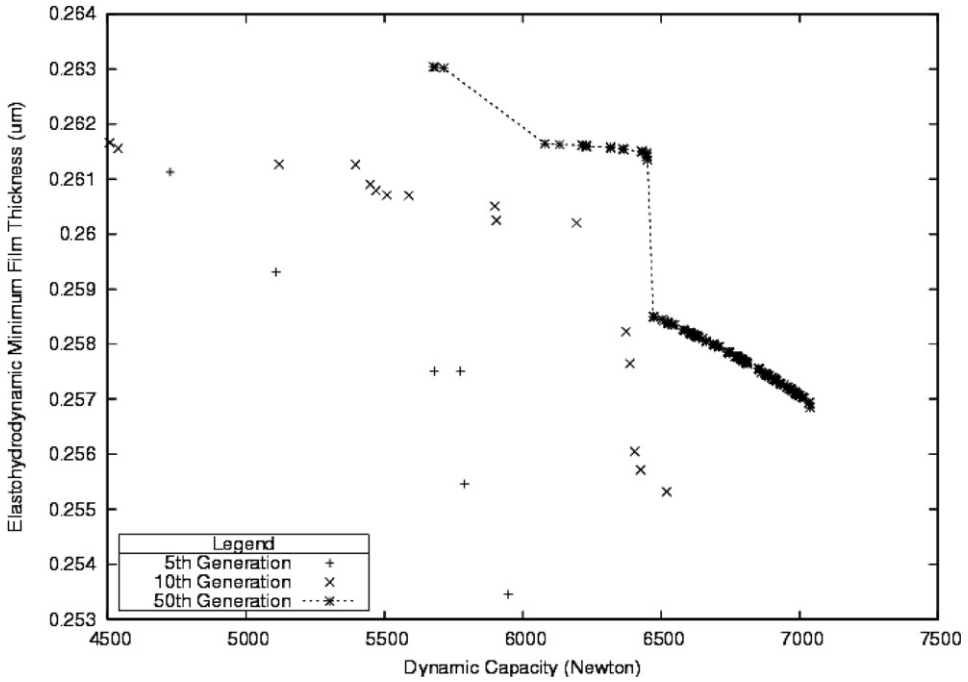

Fig. 10. Graph for simultaneous optimisation of dynamic capacity and minimum film thickness. Bearing configuration: $D = 35$ mm, $d = 15$ mm, and $B_w = 11$ mm.

- Pitch diameter (D_m): Variation in C_d and C_s is even lesser for changes in the pitch diameter (Fig. 16) when compared to their sensitivity for changes in the ball diameter. On the other hand, variation in H_{min} is slightly larger, but still less than 0.5%.

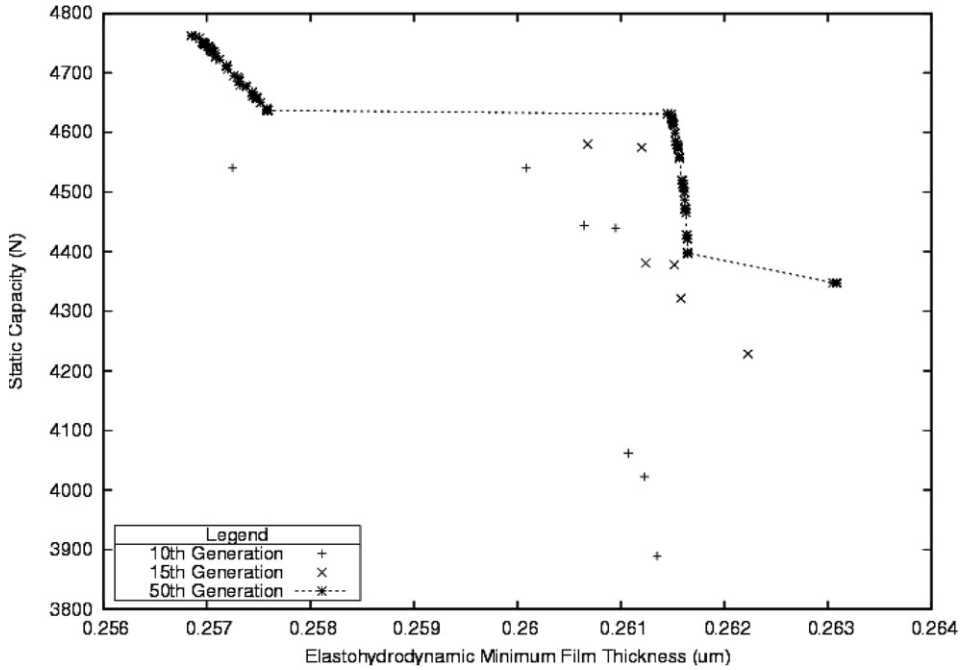

Fig. 11. Graph for simultaneous optimisation of minimum film thickness and static capacity. Bearing configuration: $D = 35$ mm, $d = 15$ mm, and $B_w = 11$ mm.

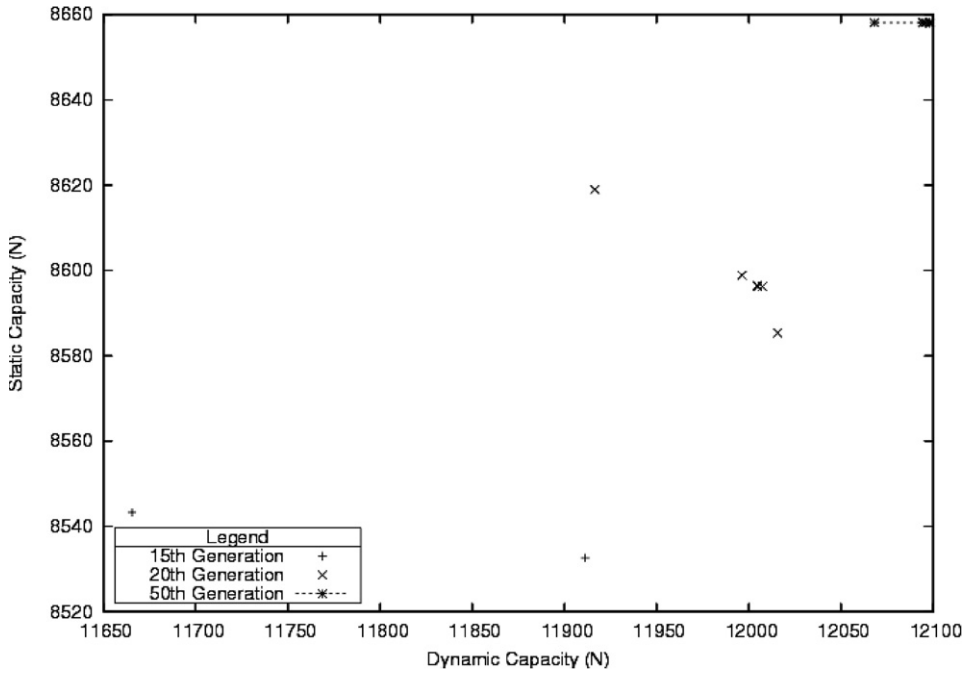

Fig. 12. Graph for simultaneous optimisation of dynamic capacity and static capacity. Bearing configuration: $D = 47$ mm, $d = 20$ mm, and $B_w = 14$ mm.

- Inner raceway curvature coefficient (f_i): Contrary to other parameters, variation in this was found to have a significant impact on the performance measures (Fig. 17). As little as 1% of variation around the optimised

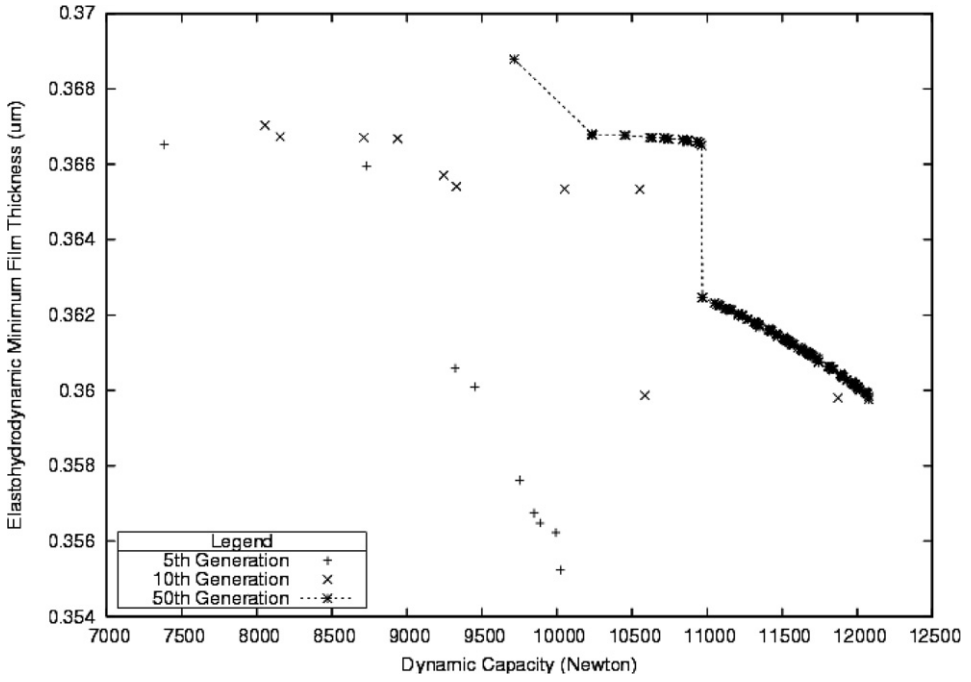

Fig. 13. Graph for simultaneous optimisation of dynamic capacity and minimum film thickness. Bearing configuration: $D = 47$ mm, $d = 20$ mm, and $B_w = 14$ mm.

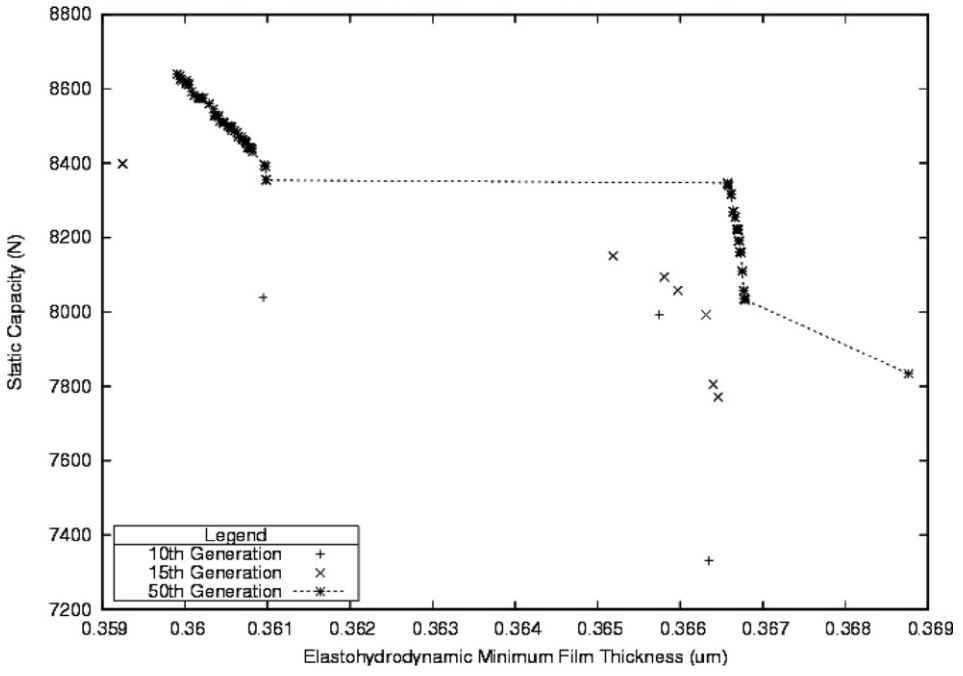

Fig. 14. Graph for simultaneous optimisation of minimum film thickness and static capacity. Bearing configuration: $D = 47$ mm, $d = 20$ mm, and $B_w = 14$ mm.

solution point led to a noticeable change 7.5% in the C_d and 12.1% change in C_s. H_{min} remained more or less unaffected from variations in this parameter.

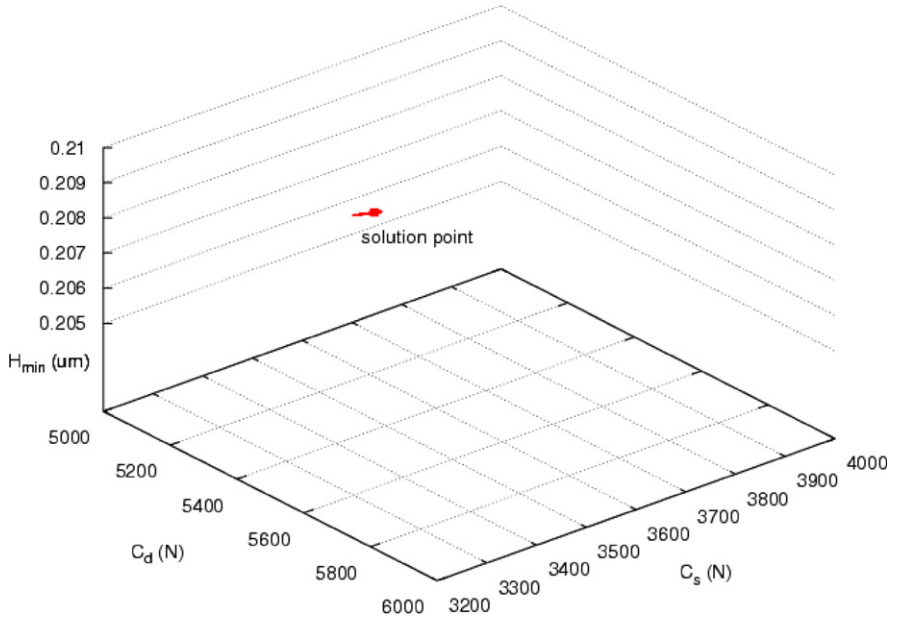

Fig. 15. Sensitivity of the performance measures around the optimised solution point: 5511.5 N (C_d), 3401.9 N (C_s), 0.2096 μm (H_{min}). Bearing configuration: $D = 30$ mm, $d = 10$ mm and $B_w = 9$ mm. This is for a maximum of ±1% variation in the ball diameter (D_b).

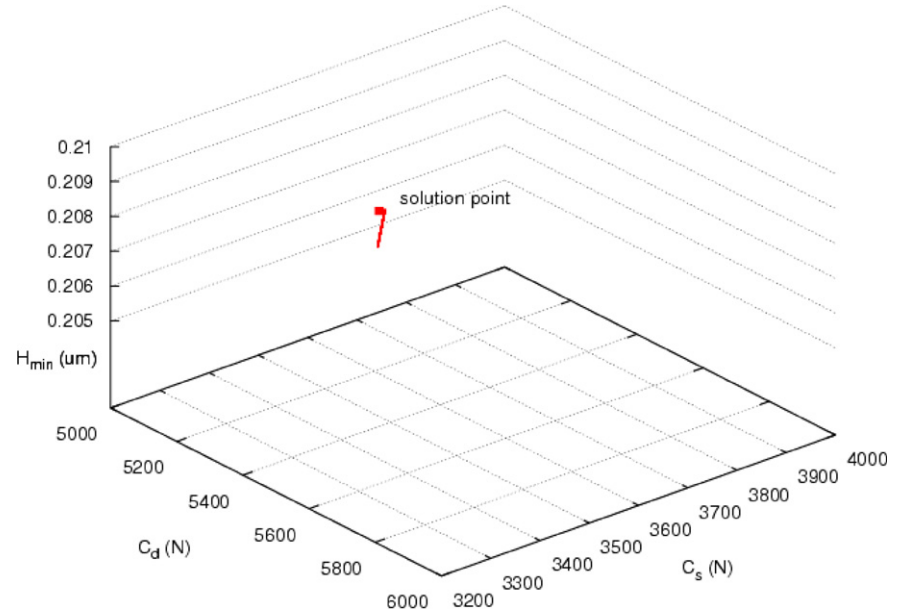

Fig. 16. Sensitivity of the performance measures around the optimised solution point: 5511.5 N (C_d), 3401.9 N (C_s), 0.2096 μm (H_{min}). Bearing configuration: $D = 30$ mm, $d = 10$ mm and $B_w = 9$ mm. This is for a maximum of ±1% variation in the pitch diameter (D_m). Variations were too small to be visible at this scale of the graph.

- Outer raceway curvature coefficient (f_o): This was found to be the least influential parameter for sensitivity analysis. It showed a marginal variation in the value of C_d, and no variation at all for C_s and H_{min} (Fig. 18).

The sensitivity analysis results are summarised in Table 10, which shows maximum variation in percentage for each of the three performance measures. One should note that these values are approximate by virtue of

Table 10
Sensitivities of performance measures C_d, C_s and H_{min} around a representative optimised solution point (bearing configuration $D = 30$, $d = 10$, $B_w = 9$; from Table 9)

	$D_b \pm 1$ (%)	$D_m \pm 1$ (%)	$f_i \pm 1$ (%)	$f_o \pm 1$ (%)	ALL ± 1 (%)	$F_r \pm 1$ (%)
C_d	0.74	0.13	7.5	0.40	7.2	0.0
C_s	0.53	0.21	12.1	0.0	11.9	0.0
H_{min}	0.07	0.43	0.02	0.0	0.52	0.047

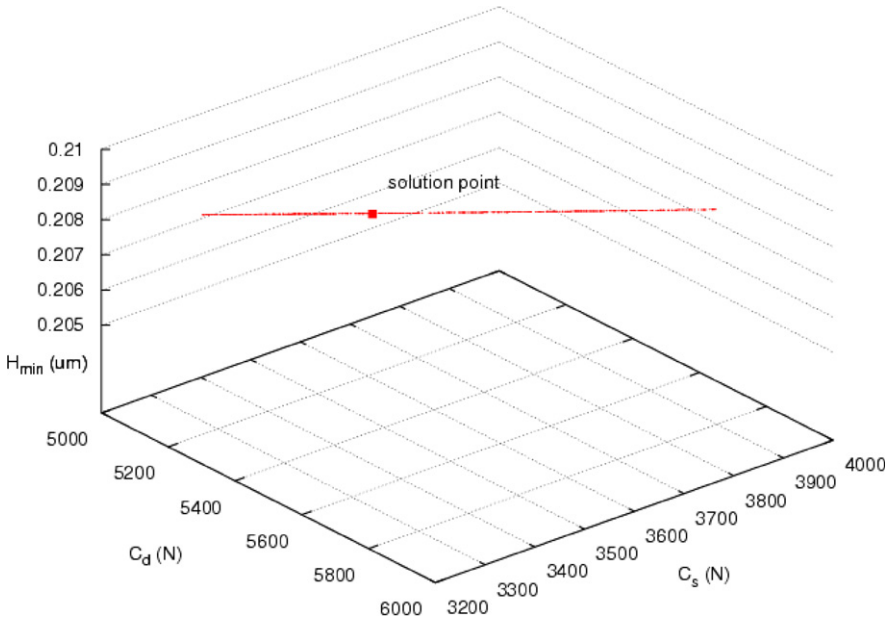

Fig. 17. Sensitivity of the performance measures around the optimised solution point: 5511.5 N (C_d), 3401.9 N (C_s), 0.2096 μm (H_{min}). Bearing configuration: $D = 30$ mm, $d = 10$ mm and $B_w = 9$ mm. This is for a maximum of ±1% variation in the inner raceway curvature coefficient (f_i).

the approach taken for sensitivity analysis (i.e. random selection of points). When all the aforementioned parameters were varied simultaneously, trend similar to a collective variation in D_m and f_i was observed. This is shown in Fig. 19. Not only do these results highlight the critical importance of the inner raceway curvature coefficient, they also demonstrate that the solutions obtained are robust against marginal parametric variations that are hard to avoid during the time of manufacture. The last column in Table 10 shows results for variation in radial load F_r which is discussed later.

Through the present optimisation runs, the parameter values of D_m and D_b having very strict digit values were obtained. In fact, manufacturing of a rolling element bearing is highly dependent on the ball diameter (D_b), the diameter parameters of inner and outer rings. Manufacture of a rolling bearing requires a good combination of these three parameters in specified tolerance ranges. The present section showed that optimised solutions are not sensitive to small variations in D_b and D_m. Hence, the inner and outer ring raceway diameters could be obtained (i.e. $(D_m - D_b)$ and $(D_m + D_b)$, respectively), considering tolerances and clearances, without much affecting the optimised solution performance. However, from the sensitivity analysis, it has been observed that performance of the bearing very much depend upon the inner groove curvature radius; and thus, it is our recommendation to practicing engineers that close tolerances must be maintain for this parameter, while manufacturing. Moreover, the experience has shown that the inner failure is the most likely cause of failure in bearings.

Another issue is that during installation of any bearing, the misalignment of 0.1–0.5° is common. Regarding the bearing misalignment, it would reflect on the equivalent radial load F_r supplied by the user based on the

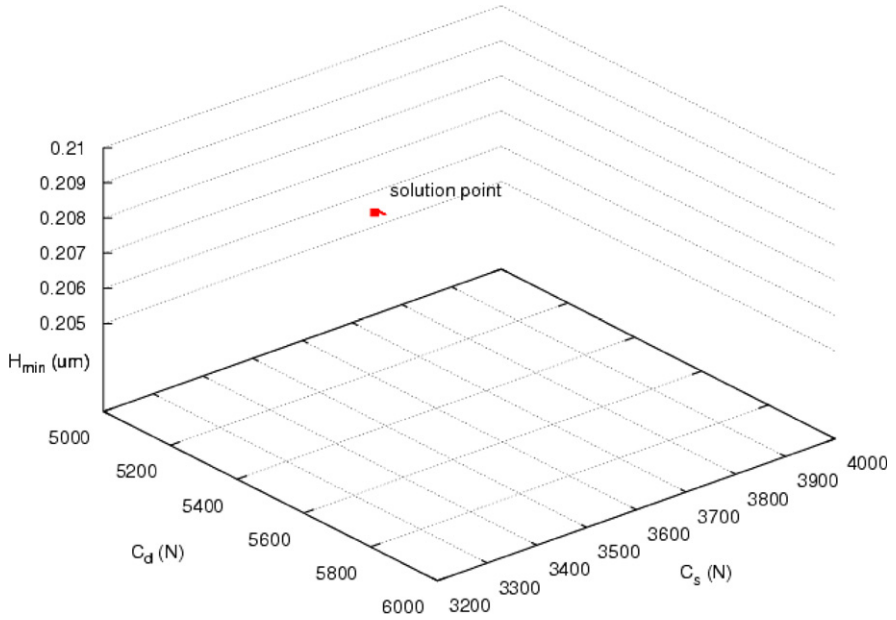

Fig. 18. Sensitivity of the performance measures around the optimised solution point: 5511.5 N (C_d), 3401.9 N (C_s), 0.2096 μm (H_{min}). Bearing configuration: $D = 30$ mm, $d = 10$ mm and $B_w = 9$ mm. This is for a maximum of ±1% variation in outer raceway curvature coefficient (f_o).

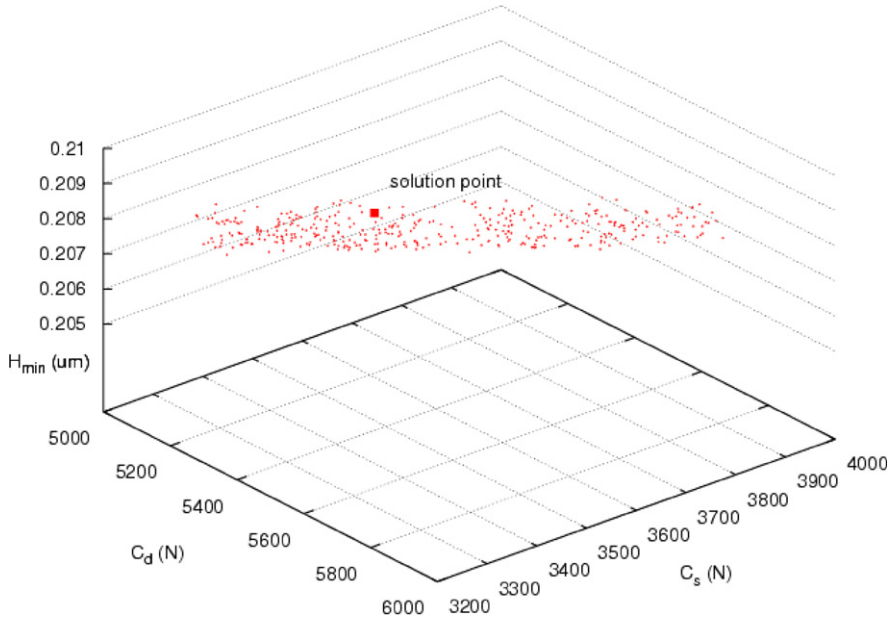

Fig. 19. Sensitivity of the performance measures around the optimised solution point: 5511.5 N (C_d), 3401.9 N (C_s), 0.2096 μm (H_{min}). Bearing configuration: $D = 30$ mm, $d = 10$ mm and $B_w = 9$ mm. This is for a maximum of ±1% variation in all four parameters D_b, D_m, (f_i) and (f_o).

operating conditions. The maximum load, Q, is related linearly with the equivalent radial load, F_r, by Eq. (10). Hence, a sensitivity analysis of the maximum load on the calculation of H_{min} has been incorporated in Appendix A, which shows that H_{min} has very little effect on the unintended misalignment during the installation. To

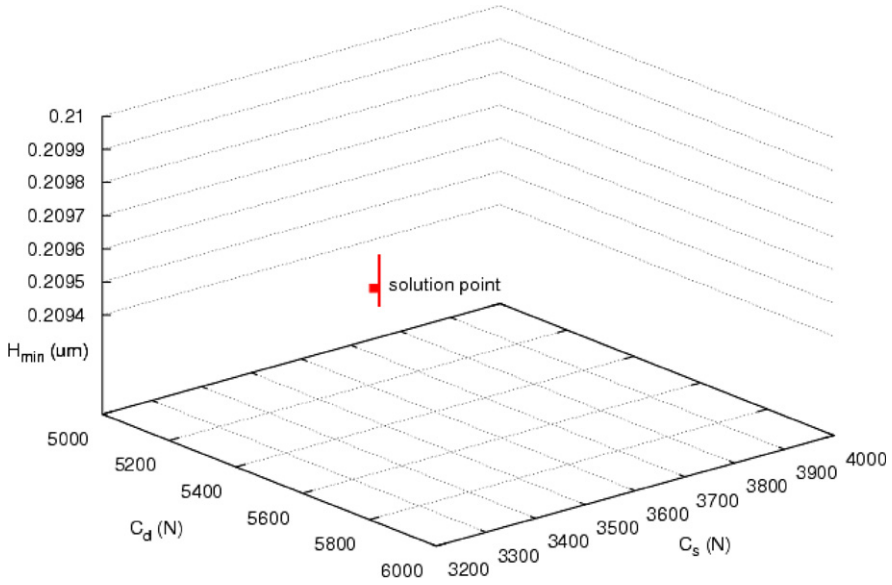

Fig. 20. Sensitivity of the performance measures around the optimised solution point: 5511.5 N (C_d), 3401.9 N (C_s), 0.2096 μm (H_{min}). Bearing configuration: $D = 30$ mm, $d = 10$ mm and $B_w = 9$ mm. This is for a maximum of ±1% variation in F_r (radial load).

further support this result, sensitivity analysis was done for variation in radial load, F_r, using the method described earlier in this section (Fig. 20). Table 10 shows that a 1% variation in the radial load leads to 0.047% change in H_{min}. This change is very close to 0.073% that is the value calculated in Appendix A for 1% variation in the radial load.

It should be noted that the minimum elastohydrodynamic film thickness has direct relevance on the choice of the roughness of the bearing components. Since in the present study this thickness is minimised, hence indirectly we are trying to suggest the best possible roughness (or in other words worst possible surface finish, which can be tolerable by practicing engineers). The surface finish is directly related with the time and cost of the production i.e. a high quality of the surface finish takes longer time and vice a versa.

5.3. Contributions

Prominent contributions of the present work that are also the drawbacks of [10]:

- K_{Dmin}, K_{Dmax}, ε, and e are included in the parameter set, allowing them to converge to the best possible values. This has been possible due to the use of robust multi-objective evolutionary optimisation algorithm.
- Multi-objective optimisation is done. This way different objective functions get optimized simultaneously. Earlier work did optimisation of dynamic capacity and altogether ignored other objectives.
- Constraint added to keep ball diameter always less than the bearing width. Absence of this had resulted in infeasible bearing designs proposed by [10].
- Constraint added to guarantee more thickness for the inner ring. In [10], most of the bearings designed had inner ring thinner as compared to the outer ring.
- Geometrically derived formula used in the present paper for calculating the value of the assembly angle $\phi_{o.}$, whereas [10] used a fixed value for the assembly angle.
- A thorough sensitivity analysis of all performance measures has been done with respect to various design parameters.
- The effect misalignment has been studied for the bearing assembly. The design has been shown to be robust against the radial load, which is related with the misalignment.

6. Conclusions

In the present paper, a procedure for the optimisation of rolling bearing design has been proposed. The optimisation problem has following characteristics: nonlinear and multi-objectives and subjected to constraints. Static and dynamic capacities and the elastohydrodynamic minimum thickness have been taken as objective functions to be maximized. Constraints are mainly kinematics in nature. The NSGA II (non-dominated sorting based genetic algorithm) has been applied to the present problem. The following conclusions can be drawn from the present results:

- The dynamic and static capacities are optimized simultaneously.
- Parameters used for constraint equations (K_{Dmin}, K_{Dmax}, ε, e) converge to a very narrow range.
- Single trade-off value (per bearing geometry) shown in tables for dual optimisation and triple optimisation is one among the several trade-off points given by the algorithm. Dual trade-offs can help in efficient design of bearings.
- Trade-off fronts might be used for studying effects of various parameters behind the calculation of dynamic and static capacities of bearings.
- Use of the geometrically accurate formula for ϕ makes calculations useful for real life bearings.
- Observation of graphs shows that at the end of each GA generation, algorithm gives out hundreds of trade-off points.
- We can perform parametric study to find out the variation in the trade-off with the changing operating conditions.
- Dynamic and static capacities has been found to be very sensitive to variations in the inner raceway curvature coefficient.

Appendix A

Nomenclature

a_{i}^*	non-dimensional major axis for the inner raceway contact
a_{o}^*	non-dimensional major axis for the outer raceway contact
b_{i}^*	non-dimensional minor axis for the inner raceway contact
b_{o}^*	non-dimensional minor axis for the outer raceway contact
B_{w}	bearing width in mm
c(p)	constraint vector
C_{d}	dynamic capacity in N
C_{s}	static capacity in N
D	bearing outer diameter in mm
D_{m}	pitch diameter in mm
D_{b}	ball diameter in mm
e	parameter for mobility conditions in Eq. (20)
E_{o}	equivalent modulus of elasticity in Pa
f_{i}	inner raceway curvature coefficient
f_{o}	outer raceway curvature coefficient
f(p)	objective vector
F_{r}	radial load in N
H_{min}	elastohydrodynamic minimum film thickness in μm
i	number of rows in the bearing
K_{Dmin}	minimum ball diameter limiter
K_{Dmax}	maximum ball diameter limiter
n_{i}	rotational speed of inner ring in rpm
p	parameter vector

r_i inner raceway groove curvature radius in mm
r_o outer raceway groove curvature radius in mm
Z number of balls
α radial contact angle in radians
α_1 pressure coefficient of viscosity in Pa^{-1}
ε parameter for outer ring strength consideration in Eq. (21)
ϕ_o assembly angle in radians
η_o dynamic viscosity at atmospheric pressure in Pa s
Z bearing width limiter
$\mathscr{P}$ parameter space
$\mathscr{F}$ objective space
$\acute{1}^n$ n-dimensional real co-ordinate space
λ coefficient for increase in bearing fatigue life

Appendix B. Sensitivity of H_{min} with Q

Eq. (8) can be expressed as

$$H_{\min,\mathrm{ring}}(Q) = CQ^{-0.073}. \tag{B.1}$$

with

$$C = 3.63a_1^{0.49}R_{x,\mathrm{ring}}^{0.466}E_o^{-0.117}\left\{\frac{\pi n_i D_m \eta_o(1-\gamma^2)}{120}\right\}^{0.68}\left[1-\exp\left\{-0.703\left(\frac{R_{(y,\mathrm{ring})}}{R_{(x,\mathrm{ring})}}\right)^{0.636}\right\}\right]. \tag{B.2}$$

Now, a small perturbation, ΔQ, on the maximum load, Q, is given, so that Eq. (B.1) becomes

$$H_{\min,\mathrm{ring}}(Q+\Delta Q) = C(Q+\Delta Q)^{-0.073} \approx CQ^{-0.073} + \frac{\partial(CQ^{-0.073})}{\partial Q}\Delta Q. \tag{B.3}$$

Equation can be rearranged as

$$\frac{H_{\min,\mathrm{ring}}(Q+\Delta Q) - H_{\min,\mathrm{ring}}(Q)}{H_{\min,\mathrm{ring}}(Q)} = \frac{1}{CQ^{-0.073}}\frac{\partial(CQ^{-0.073})}{\partial Q}\Delta Q = -0.073\frac{\Delta Q}{Q}. \tag{B.4}$$

It should be noted that 1% change in the maximum load would change minimum elastohydrodynamic thickness by 0.073% and 5% change in the load would change the thickness by 0.365%.

References

[1] M. Asimow, Introduction to Engineering Design, McGraw Hill, New York, 1966.
[2] A. Seireg, H. Ezzat, Optimum design of hydrodynamic journal bearings, Transactions of ASME, Journal of Lubrication Technology 91 (3) (1969) 516–523.
[3] C.J. Maday, The maximum principle approach to the optimum one-dimensional journal bearing, Transactions of ASME, Journal of Lubrication Technology 92 (2) (1970) 482–489.
[4] G.M. Wylie, C.J. Maday, The optimum one-dimensional hydrodynamic gas Rayleigh step bearing, Transactions of ASME, Journal of Lubrication Technology 92 (3) (1970) 504–508.
[5] A. Seireg, A survey of optimisation of mechanical design, Transactions of ASME, Journal of Engineering for Industry 94 (2) (1972) 495–599.
[6] H. Hirani, K. Athre, S. Biswas, Comprehensive design methodology for an engine journal bearing, Proceedings of Institution of Mechanical Engineers, Part J 214 (2000) 401–412.
[7] W. Changsen, Analysis of Rolling Element Bearings, Mechanical Engineering Publications Ltd, London, 1991.
[8] D.H. Choi, K.C. Yoon, A design method of an automotive wheel bearing unit with discrete design variables using genetic algorithms, Transactions of ASME, Journal of Tribology 123 (1) (2001) 181–187.
[9] P. Periaux, Genetic Algorithms in Aeronautics and Turbomachinery, Wiley, New York, 2002.
[10] I. Chakraborthy, K. Vinay, S.B. Nair, R. Tiwari, Rolling element bearing design through genetic algorithms, Engineering Optimisation 35 (6) (2003) 649–659.

[11] B.R. Rao, R. Tiwari, Optimum design of rolling element bearings using genetic algorithms, Mechanism and Machine Theory 42 (2) (2007) 233–250.
[12] K. Kalita, R. Tiwari, S.K. Kakoty, Multi-Objective Optimisation in rolling element bearing system design, in: Proceedings of the International Conference on Optimisation SIGOPT 2002, February 17–22, Lambrecht, Germany, 2002.
[13] C.C.A. Coello, Handling Preferences in Evolutionary Multi-Objective Optimisation: A Survey. Congress on Evolutionary Computation, vol. 1, IEEE Service Center, Piscataway, NJ, Julio del 2000, 2000, pp. 30–37.
[14] E. Zitzler, Evolutionary Algorithms for Multi-objective Optimisation: Methods and Application, Ph.D. thesis, Swiss Federal Institute of Technology (ETH), Aachen, Germany, 1999.
[15] K. Deb, S. Agrawal, A. Pratap, T. Meyarivan, A fast elitist non-dominated sorting genetic algorithm for multi-objective optimisation: NSGA-II, in: Proceedings of the Parallel Problem Solving from Nature VI Conference, Paris, France, Lecture Notes in Computer Science No. 1917, Springer, 2000, pp. 849–858.
[16] K. Miettinen, Nonlinear Multi-objective Optimisation, Kluwer Academic Publishers, Boston, 1999.
[17] K. Deb, Multi-objective Optimisation Using Evolutionary Algorithms, Wiley–Interscience Series in Systems and Optimisation, New York, 2001.
[18] J. Andersson, Multi-objective Optimisation in Engineering Design: Applications to Fluid Power Systems, Ph.D. Thesis, Division of Fluid and Mechanical Engineering Systems, Department of Mechanical Engineering, Linkopings University, Sweden, 2001.
[19] J.E. Shigley, C.R. Mischke, Mechanical Engineering Design, McGraw-Hill Book Company, New York, 1989.
[20] KanGAL (Kanpur Genetic Algorithm Laboratory), Indian Institute of Technology Kanpur, India. http://www.iitk.ac.in/kangal/.